DOI: 10.1002/cbic.200500064

Stochastic Sensing of TNT with a Genetically Engineered Pore

Xiyun Guan,[a] Li-Qun Gu,[b] Stephen Cheley,[a] Orit Braha,[c] and Hagan Bayley*[c]

Engineered versions of the transmembrane protein pore α-hemolysin (αHL) can be used as stochastic sensing elements for the identification and quantification of a wide variety of analytes at the single-molecule level. Until now, nitroaromatic analytes have eluded detection by this approach. We now report that binding sites for nitroaromatics can be built within the lumen of the αHL pore from simple rings of seven aromatic amino acid side chains (Phe, Tyr or Trp). By monitoring the ionic current that passes through a single pore at a fixed applied potential, various nitroaromatics can be distinguished from TNT on the basis of the amplitude and duration of individual current-blocking events. Rings of less than seven aromatics bind the analytes more weakly; this suggests that direct aromatic–aromatic interactions are involved. The engineered pores should be useful for the detection of explosives and, in combination with computational approaches and structural analysis, they could further our understanding of noncovalent interactions between aromatic molecules.

Introduction

Stochastic sensors detect analytes at the single-molecule level.[1–3] Engineered versions of the transmembrane protein pore α-hemolysin (αHL) have been used as stochastic sensing elements for the identification and quantification of a wide variety of substances, including metal ions,[4,5] anions,[6] organic molecules,[7] reactive molecules,[8] DNA[9] and proteins.[10] In this approach, binding sites for analytes are usually engineered within the lumen of the pore. The ionic current passing through a single pore is monitored at a fixed applied potential. Individual binding events are detected as transient blockades in the recorded current. This allows both the identification and quantification of analytes. We now report that nitroaromatic molecules can be detected at the single-molecule level by using rings of aromatic residues placed at a key site within the lumen of αHL. Various nitroaromatics are distinguished from 2,4,6-trinitrotoluene (TNT) on the basis of the amplitude and duration of current block. This finding should be useful for the detection of explosives and could further our understanding of noncovalent interactions between aromatic molecules.

Results and Discussion

Engineered αHL pores with internal aromatic rings

Aromatic side chains were introduced at position 113 of the αHL polypeptide by site-directed mutagenesis, and pores were assembled from the mutant subunits. The heptameric mutant pores[11] therefore contained seven aromatic side chains that projected into the lumen at the top of the transmembrane β barrel (Figure 1). Residue 113 is close to the narrowest part of the lumen. Therefore, it seemed likely that analyte molecules that bind near that site would affect the transmembrane current.

Nitroaromatics block the engineered pores

To monitor interactions between the mutant pores and nitroaromatic analytes, single-channel current recordings were made in a planar bilayer apparatus. For example, TNT was tested with the mutant pore, Met113Trp$_7$. In the absence of an analyte, the pore remained open at all times and exhibited a unitary conductance of 643 ± 7 pS ($n = 4$). In the presence of TNT, both short and long current blockades were observed (Figure 2A). The long events lasted about one second, and during this period the pore was almost completely blocked (residual conductance of 28 ± 2 pS, $n = 3$). A plot of $1/\tau_{on}$ as a function of TNT concentration for Met113Trp$_7$ is linear (Figure 2B), where τ_{on} is the mean inter-event interval (ignoring the short events). This suggests that the long interaction is bimolecular.[12,13] A K_d value was obtained for the long events (Table 1) by using $k_{off} = 1/\tau_{off}$ and $k_{on} = 1/(\tau_{on} \cdot [TNT])$,[12,13] where τ_{off} is the mean dwell time of a TNT molecule in the protein. Although τ_{off} approaches 1 s, the K_d value is only ~1 mM. This is because the association rate constant is surprisingly slow, $\sim 10^3\ M^{-1}\ s^{-1}$, compared to most rate constants we have

[a] Dr. X. Guan, Dr. S. Cheley
Department of Medical Biochemistry & Genetics
The Texas A&M University System Health Science Center
College Station, Texas 77843-1114 (USA)

[b] Dr. L.-Q. Gu
Department of Biological Engineering
Dalton Cardiovascular Research Center, University of Missouri
Columbia, MO 65211 (USA)

[c] Dr. O. Braha, Dr. H. Bayley
Department of Chemistry, University of Oxford
Mansfield Road, Oxford, OX1 3TA (UK)
Fax: (+44) 1865-275708
E-mail: hagan.bayley@chem.ox.ac.uk

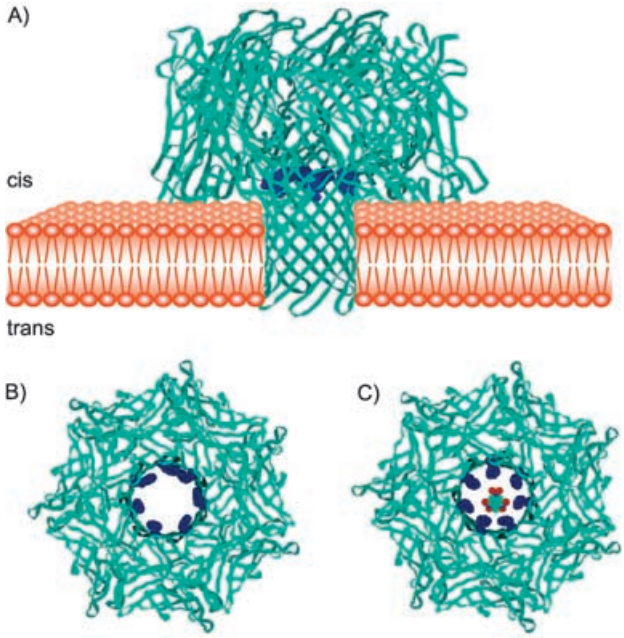

Figure 1. Molecular graphics representations of the staphylococcal αHL pore. A) Side view of the Met113Phe$_7$ pore highlighting position 113, where the naturally occurring Met residue has been substituted with Phe (blue). B) View into the Met113Phe$_7$ pore from the cis side of the lipid bilayer. C) View into the Met113Phe$_7$ pore showing a TNT molecule at the same scale. The Phe side chains are shown in extended conformations and the TNT molecule has been placed with the plane of the ring perpendicular to the central axis of symmetry in the pore.

determined for small molecules that bind within αHL, $>10^5\ M^{-1}s^{-1}$.[4,6,7,12]

Long binding events

To investigate the origin of the long events, αHL pores assembled from additional Met113 mutants were tested with TNT.

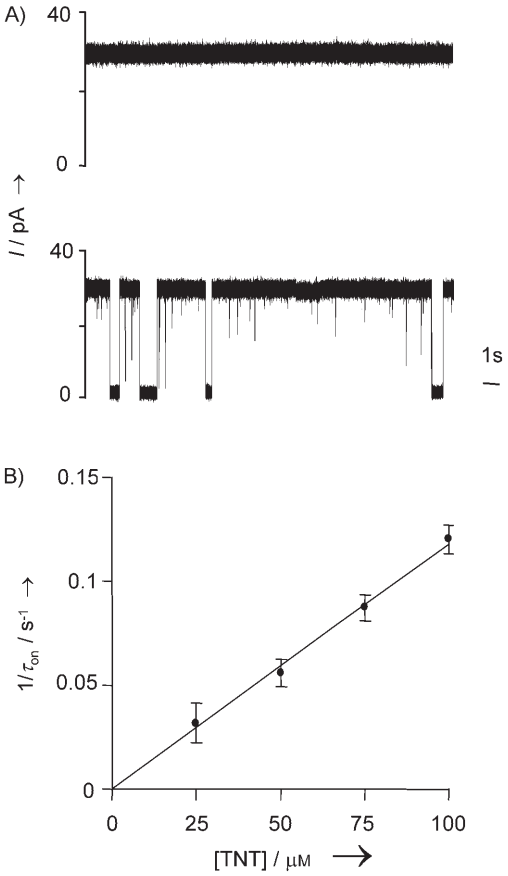

Figure 2. Interaction of TNT with a single Met113Trp$_7$ pore. A) Upper panel: current trace in the absence of TNT; lower panel: current trace in the presence of 50 μM TNT. The TNT was added to the chamber (1.52 mL) in acetonitrile (17.2 μL). The same volume of acetonitrile was included in the experiment shown in the upper trace. B) Plot of $1/\tau_{on}$ as a function of TNT concentration. The calculation of $1/\tau_{on}$ ($n=3$) was based on the long blocking events. Experiments were performed at +50 mV (cis at ground) in NaCl (1 M), Tris·HCl (10 mM, pH 7.5). Both Met113Trp$_7$ and TNT were added to the cis chamber.

Table 1. Characteristics of binding events between TNT and homoheptameric αHL pores.[a]

Mutant[b] pore	Amino-acid side chain at position 113	Residual conductance [pS][c]	Residual conductance [%][d]	τ_{off} [ms]	k_{on} [$M^{-1}s^{-1}$]	K_d [M]
Met113Trp$_7$	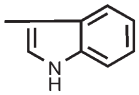	28 ± 2	4.3	820 ± 40	900 ± 70	$1.4 \pm 0.1 \times 10^{-3}$
Met113Phe$_7$[e]	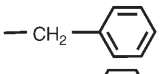	41 ± 8	5.6	300 ± 40	540 ± 70	$6.1 \pm 0.4 \times 10^{-3}$
Met113Tyr$_7$	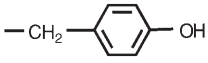	28 ± 3	3.8	1030 ± 50	620 ± 70	$1.6 \pm 0.1 \times 10^{-3}$

[a] Experiments were performed in NaCl (1 M), Tris·HCl (10 mM, pH 7.5) at an applied potential of +50 mV. Both αHL protein and TNT (50 μM) were added to the cis chamber. τ_{off}, k_{on} and K_d values were calculated for the long blocking events and are based on three separate experiments (mean ± standard deviation). When the TNT was in the cis chamber, there were no blocking events at −50 mV. However, with TNT in the trans chamber, blocking events were observed at −50 mV and not at +50 mV. The events with TNT on the trans side had smaller τ_{off} values compared to those seen with TNT on the cis side (e.g., about 100 ms for Met113Trp$_7$). [b] The following pores were also tested: WT$_7$, Met113His$_7$, Met113Asp$_7$, Met113Glu$_7$, Met113Arg$_7$, Met113Lys$_7$, Met113Val$_7$ and Met113Pro$_7$. Neither short nor long blocking events were observed in these cases. [c] The residual conductance during the long blocking events calculated on the basis of the remaining current in a single channel experiment. [d] The residual conductance during the long blocking events as a percentage of the unitary conductance. The open channel conductances for mutants Met113Trp$_7$, Met113Phe$_7$ and Met113Tyr$_7$ were 643 ± 7 pS, 732 ± 14 pS and 742 ± 2 pS, respectively. [e] The experiment with Met113Phe$_7$ was repeated with a high purity sample of TNT from Supelco (99.9%), yielding values of τ_{off} = 290 ms and $k_{on} = 510\ M^{-1}s^{-1}$.

These mutants included Met113Phe$_7$, Met113Tyr$_7$, Met113His$_7$, Met113Asp$_7$, Met113Glu$_7$, Met113Arg$_7$, Met113Lys$_7$, Met113Pro$_7$ and Met113Val$_7$. The new amino acid residues in the mutants belonged to three major classes: hydrophobic (Met, Pro, Val), charged (Asp, Glu, Arg, Lys) and aromatic (Trp, Phe, Tyr). Current blocking events were identified only with the three aromatic Met113 mutants (Table 1); this argues against a general hydrophobic interaction. The failure of the charged side chains to bind TNT argues against cation–π[14] or anion–π[15] interactions in these cases. Aromatic–aromatic interactions involving histidine residues have been reported.[16–18] However, TNT did not block Met113His$_7$ at pH 7.5 or pH 9.5, at which the His residues are likely to be fully deprotonated.

It is probable then that TNT interacts directly with aromatic side chains within the lumen of the pore. The interaction between TNT and Trp, Tyr and Phe might have donor–acceptor character. The ring in TNT is electron deficient, while those in Tyr and Trp are electron rich, compared with the ring in Phe. Our results yield a binding strength in the order Tyr ~ Trp > Phe (Table 1). This is similar to observations made for the binding of 7-methylguanosine to aromatic side chains in the mRNA "cap" binding proteins, eIF4E and VP39, where face-to-face π-stacking interactions occur.[19] However, there is no direct evidence that π stacking occurs in the present case.

Origin of the short and long binding events

The short events exhibited a wide range of amplitudes (Figure 2A). Nevertheless, a rough value for τ_{off} could be determined by fitting a dwell-time histogram to a single exponential ($\tau_{off} = 0.67 \pm 0.05$ ms, $n = 3$). To investigate the origin of the short and long events, a series of heteromeric Met113Phe pores were assembled and examined by current recording. These included Met113Phe$_1$WT$_6$, Met113Phe$_2$WT$_5$ and Met113Phe$_3$WT$_4$ throught to Met113Phe$_7$, where WT is the wild-type subunit (Figure 3). τ_{on} and τ_{off} values were determined, and $\Delta G°$ values for the short and long events were estimated by using $\Delta G° = -RT \ln K_f$ (Figure 4). As the ratio of Met113Phe to WT subunits increased, τ_{off} for the long binding events also increased exponentially, while $1/\tau_{on}$ at a fixed TNT concentration was almost unchanged (Figure 4A and B). By contrast, τ_{off} for the short binding events was independent of the subunit ratio, while $1/\tau_{on}$ increased from 0.025 s^{-1} to 0.44 s^{-1} at 50 μM TNT as the Met113Phe to WT ratio increased (Figure 4D and E). For both the short and long events, $\Delta G°$ decreased roughly linearly with the number of Met113Phe subunits (Figure 4C and F). For the

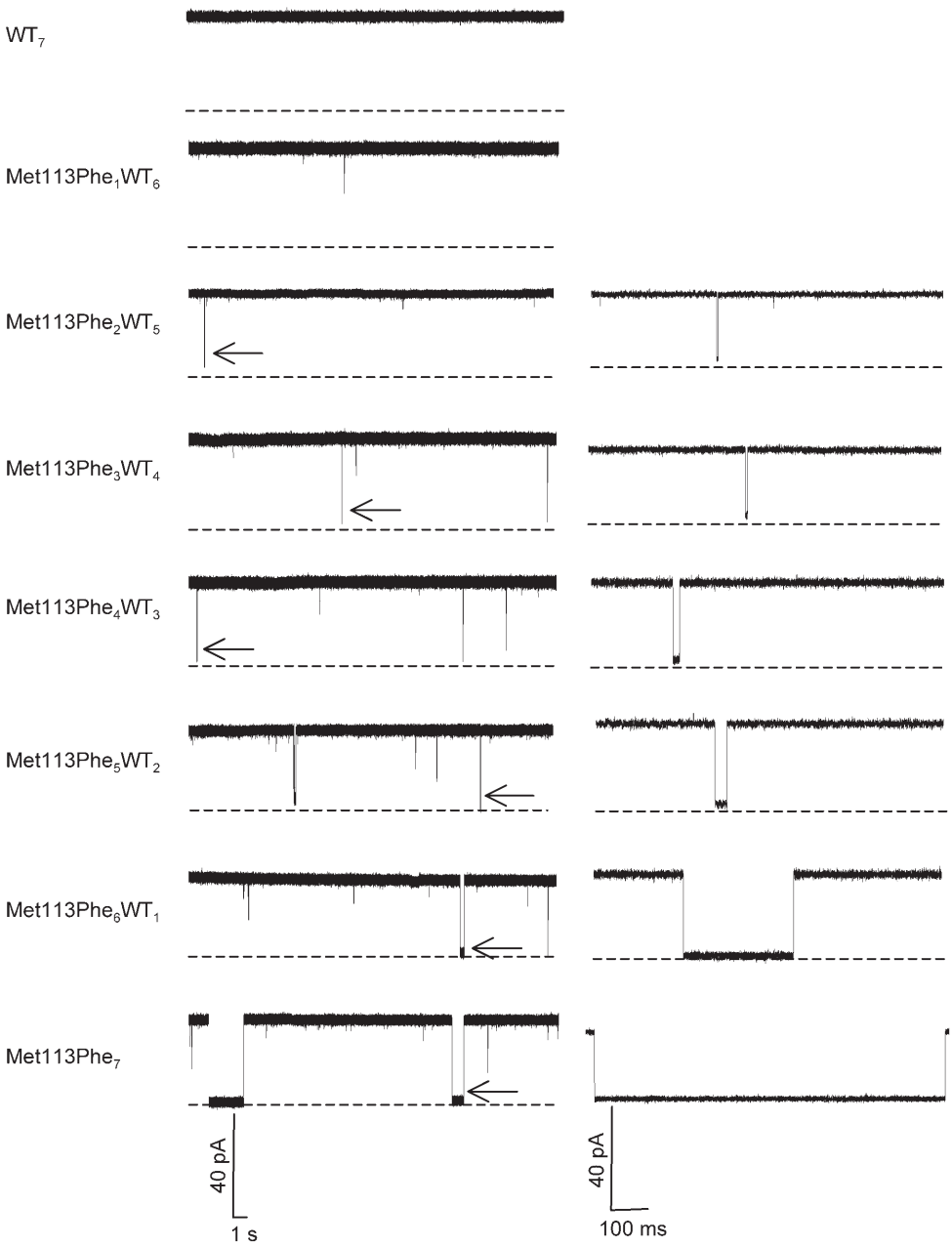

Figure 3. Single-channel recordings with a series of Met113Phe mutants that show short and long events caused by the binding of TNT. The left-hand traces are 30 s in duration. The right-hand traces are 1 s in duration and show expanded views of the long events marked with arrows on the left. The broken lines are at zero current. The experiments were performed at +50 mV in NaCl (1 M), Tris·HCl (10 mM, pH 7.5). Both Met113Phe proteins and TNT (50 μM) were added to the cis chamber.

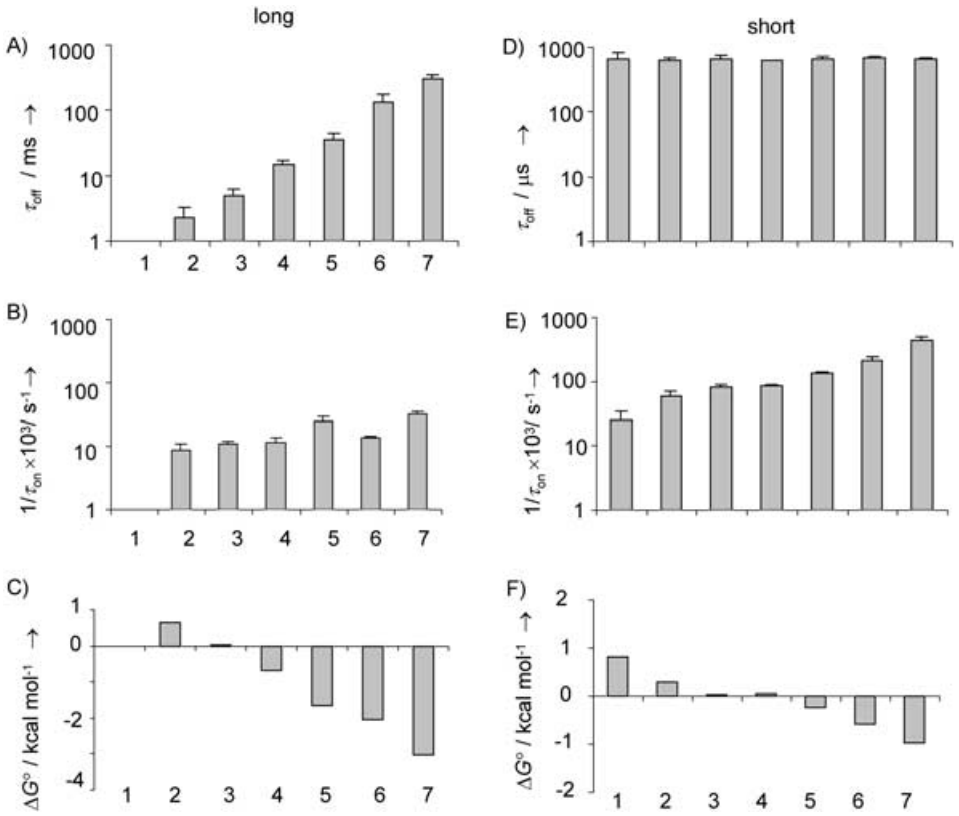

Figure 4. The effect of the number of Phe residues in the Met113Phe mutant pores on TNT (50 µM) binding. 1, Met113Phe$_1$WT$_6$; 2, Met113Phe$_2$WT$_5$; 3, Met113Phe$_3$WT$_4$; 4, Met113Phe$_4$WT$_3$; 5, Met113Phe$_5$WT$_2$; 6, Met113Phe$_6$WT$_1$; 7, Met113Phe$_7$. A–C) τ_{off}, $1/\tau_{on}$ and $\Delta G°$ values for the long events. D–F) τ_{off}, $1/\tau_{on}$ and $\Delta G°$ values for the short events.

short events, both the overall decrease in $\Delta G°$ (−1.8 kcal mol^{-1}) and the overall change in $1/\tau_{on}$ (18-fold) are somewhat larger than the values expected from a purely statistical effect based on an increase in individual binding sites from one to seven per pore ($\Delta\Delta G° = -RT\ln 7 = -1.1$ kcal mol^{-1}; change in $1/\tau_{on}$ = sevenfold). These data suggest that the short events are primarily related to interactions between single Phe residues and a TNT molecule, while the long events require at least two Phe residues.

The examination of a series of analytes with the Met113Trp$_7$ pore provided further evidence that the binding events arise from direct aromatic–aromatic interactions between the amino acid side chains and the analyte molecules (Table 2). All six nitroaromatics tested bound to Met113Trp$_7$. The affinity dropped off for molecules with

Table 2. Interaction of various organic analytes with the Met113Trp$_7$ pore.[a]

Analyte	Structure	Residual conductance [pS][b]	Residual conductance [%][c]	τ_{off} [ms]	k_{on} [M^{-1} s^{-1}]	K_d [M]
TNT	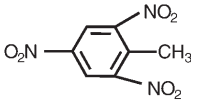	28 ± 2	4.3	820 ± 40	900 ± 70	$1.4 \pm 0.1 \times 10^{-3}$
Tetryl	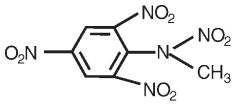	20 ± 1	3.1	150 ± 40	120 ± 20	$5.5 \pm 0.1 \times 10^{-2}$
2,6-DNT	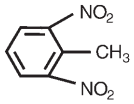	92 ± 3	14	14 ± 2	17 ± 3	4.4 ± 0.8
2,4-DNT	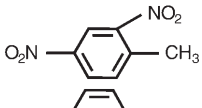	100 ± 10	16	13 ± 4	23 ± 5	3.2 ± 1.0
4-NT		140 ± 10	22	1.8 ± 0.9	19 ± 4	32 ± 9
4-amino-DNT	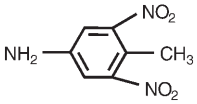	100 ± 10	16	3.7 ± 0.8	22 ± 2	13 ± 3

[a] Experiments were performed in NaCl (1 M), Tris·HCl (10 mM, pH 7.5) at an applied potential of +50 mV. Both αHL protein and nitroaromatics (50 µM–1 mM) were added to the cis chamber. τ_{off}, k_{on} and K_d values were calculated for the long blocking events and are based on three separate experiments (mean ± standard deviation). Short events were also observed with TNT, Tetryl, 2,6-dinitrotoluene (2,6-DNT), 2,4-dinitrotoluene (2,4-DNT), 4-nitrotoluene (4-NT) and 4-amino-2,6-dinitrotoluene (4-amino-DNT). [b] The residual conductance during the long blocking events calculated on the basis of the remaining current in a single-channel experiment. [c] The residual conductance during the long blocking events as a percentage of the unitary conductance.

fewer nitro groups, which is in accordance with the idea of a donor–acceptor interaction. The nonaromatic nitro explosive hexahydro-1,3,5-trinitro-1,3,5-triazine (RDX) did not interact with the pore.

Mechanism of current block

Our results suggest that the long binding events between the mutant αHL pores and TNT and its relatives have a stoichiometry of 1:1 (Figure 2B). The results also indicate that the Phe, Tyr or Trp residues cooperate in the long interactions. However, it is hard to reconcile the almost complete channel block seen upon binding of TNT and related molecules with the dimensions of the lumen, as seen in the crystal structure of the unoccupied pore (Figure 1). A substantial current block of the pore does not require complete occlusion of the lumen. First, in a wide pore, hydrated ions are transported. Once the diameter of the aperture is reduced below 5 or 6 Å, water molecules must be stripped from the ions before they can move though the lumen.[20] The high energetic cost would greatly retard transport in the absence of any compensating factors. Second, exclusion of solvent could occur in a narrow hydrophobic channel, thus reducing the mean current.[21] Nevertheless, when a TNT molecule (diameter ~7 Å) is placed within the lumen of the αHL pore with the aromatic ring perpendicular to the central axis, it is hard to envision the bonding interactions that would be required to maintain its position for ~1 s, even if the side chains of the aromatic residues at position 113 are placed in their most extended conformations (Figure 1). It is worth comparing the interactions of the larger βCD (outer diameter ~15 Å) with $Met113Phe_7$ pores.[12] The residual current in this case is 26%, far larger than in the case of TNT. Several lines of evidence suggest that the cyclodextrin is oriented with its central axis coincident with the central axis of the pore, and the latter is in a conformation closely similar to that determined by crystallography.[7] Therefore, hydrated ions flow through the central cavity of the cyclodextrin, which is ~6 Å in diameter. A second striking difference is that k_{on} for the more bulky βCD ($3.1\times10^5\ M^{-1}\ s^{-1}$)[12] is far greater than that for TNT. It seems possible then that TNT binds to and stabilizes a rare conformational state of the pore. Normally, this state must be short lived because it is not observed in single-channel recordings of the pores in the absence of TNT.

While we have little information that would allow us to make a molecular representation of the αHL–TNT complex, it is still possible to speculate on the nature of the interaction. Aromatic–aromatic interactions remain an area of active investigation and occur in T-shaped (edge-to-face), offset-stacked and stacked geometries.[22–24] The augmentation of these interactions in clusters of aromatics, as seen here, where ~0.74 kcal mol^{-1} are provided per Phe residue (Figure 4), is also well documented.[22–24] Multiple T-shaped interactions (as suggested by Figure 1, but there the distances are too great) would require a conformational change of modest magnitude. An inward movement of ~1.5 Å by each Phe residue would produce an appropriate centroid (of the Phe ring) to edge (TNT) distance of 3.5 Å. However, the interactions investigated here have a discernible donor–acceptor character: the Trp and Tyr mutants bind TNT better than the Phe mutant (Table 1), and the more heavily nitrated aromatics have greater affinity for the pores (Table 2). Further, the edge interactions that would be mediated by aromatic CH groups in an electron-deficient ring are sterically blocked by the arrangement of the nitro groups in TNT. Therefore, a stacked interaction is most likely, but it would require a more radical conformational change, for example, a partial collapse of the upper part of the barrel to form an aromatic cluster.[16,25]

Conclusion

The ability to detect individual nitroaromatic molecules has several potential applications in biotechnology. A notable possibility is in the detection of explosives. TNT is a high explosive used in military and industrial applications. It is also a priority pollutant listed by the US Environmental Protection Agency.[26,27] Traditional methods for the analysis of TNT include HPLC combined with various detection methods such as mass spectrometry.[26] Additional methods include the quenching of fluorescence in conjugated polymer films,[28–30] the detection of deflagration on a microcantilever[31] and binding to engineered fluorescent proteins.[32] Single-molecule detection, as demonstrated here, has potential advantages. For example, related nitroaromatic compounds have different current signatures with the same sensor element (Table 2). This allows the constituents of a mixture to be identified.[5,7] The polymers that are used in some sensors cannot distinguish between different nitroaromatics.[28,29] In this context, it should be noted that TNT has several important nitroaromatic breakdown products, including 2,4-dinitrotoluene[33] and 4-*N*-acetylamino-2-amino-6-nitrotoluene,[27] the distribution of which depends on the environment. Components of the current signatures include the τ_{off} value, the extent of current block and the ratio of long to short binding events. The present limit for rapid detection of TNT with $Met113Trp_7$, arbitrarily defined as three long binding events in a 1 min recording, is ~50 μM. Clearly, improved protein engineering is required to lower this limit. Based on our interpretation of the long binding events, the development of pores with tighter internal constrictions to provide preformed aromatic clusters should help.

With further development, single-molecule detection could also promote our fundamental understanding of aromatic interactions, which are important in many areas. For example, aromatic interactions are involved in the folding and stability of proteins.[16,25,34–36] In principle, the system we have developed permits the kinetic analysis of aromatic interactions in a defined environment under a wide range of aqueous conditions. Nevertheless, to profit fully from such work, computational studies and structural information about the mutant pores and their complexes with molecules such as TNT would be required. Such studies have been highly informative in related investigations of soluble proteins.[19,32,37,38]

Experimental Section

Materials: TNT, methyl-2,4,6-trinitrophenylnitramine (Tetryl), RDX, 2,4-dinitrotoluene, 2,6-dinitrotoluene, 4-nitrotoluene and 4-amino-2,6-dinitrotoluene were obtained from Cerilliant Corporation (Round Rock, Texas, USA). An additional sample of high purity TNT (99.9%) was obtained from Supelco (Bellefonte, PA, USA). Stock solutions (1 mg mL^{-1}) were in acetonitrile. All other reagents were purchased from Sigma.

Protein engineering: Mutant αHL genes were constructed by cassette mutagenesis with a previously remodelled gene in a T7 vector (pT7–αHL-RL2), which has been described elsewhere.[12] Homoheptameric wild-type αHL and mutant αHL pores were assembled as described previously.[12] The heteroheptameric Met113Phe pores were obtained by coassembling Met113Phe and WT-D8 αHL subunits in various ratios on rabbit erythrocyte membranes. The resulting heptamers, Met113Phe$_1$WT$_6$, Met113Phe$_2$WT$_5$, Met113Phe$_3$WT$_4$ through to Met113Phe$_7$, were separated based on their different gel shifts, which were caused by the C-terminal extensions of eight Asp residues (the "D8" tail).[9]

Current recordings: A bilayer of 1,2-diphytanoylphosphatidylcholine (Avanti Polar Lipids; Alabaster, AL, USA) was formed on an aperture (120 μm) in a Teflon septum (25 μm thick; Goodfellow, Malvern, PA, USA) that divided a planar bilayer chamber into two compartments, cis and trans. Each compartment contained buffer (1.5 mL) comprising NaCl (1 M), Tris·HCl (10 mM, pH 7.5) at 22 ± 1 °C. Unless otherwise noted, both the αHL protein and the analyte in acetonitrile were added to the cis compartment, which was connected to "ground". Control experiments with acetonitrile (up to 40 μL per chamber) were done in the same way. The final concentration of the αHL protein was 0.2–2.0 ng mL^{-1}. The applied potential was +50 mV. We ruled out two potential difficulties that might have produced misleadingly low values for k_{on}. First, it was possible that an impurity in the TNT produced the binding events. The experiments were therefore repeated with a highly purified batch of TNT with similar results (Table 1). Second, it was possible that the TNT quickly adsorbed onto the surface of the bilayer apparatus. Therefore, the concentration of the TNT in the chamber was checked after an experiment by UV-visible absorption spectroscopy, and found to be unchanged. Currents were recorded with a patch clamp amplifier (Axopatch 200B, Axon Instruments; Foster City, CA, USA). They were low-pass filtered with a built-in four-pole Bessel filter at 10 kHz, which was appropriate for obtaining the amplitude and τ_{off} of the short events. Finally, they were sampled at 20 kHz by a computer equipped with a Digidata 1200 A/D converter (Axon Instruments).

Data analysis: Data were analyzed with the following software: pClamp 7.0 (Axon Instruments), Clampfit 9.0 (Axon Instruments) and Microsoft Excel 2000. Single-channel current amplitude and dwell time histograms were constructed with Clampex 7.0 (Axon Instruments). Conductance values were obtained from the amplitude histograms after the peaks were fit to Gaussian functions. Mean residence times (τ values) for the analytes were obtained from dwell time histograms by fitting the distributions to exponential functions. To determine kinetic constants, three separate experiments were performed in each case, and data were acquired for at least 10 min in each experiment.

Molecular modelling: The model of Met113Phe$_7$ was derived from the structure of the wild-type αHL pore (PDB: 7AHL) with the "mutate" and/or "tor" functions of SPOCK 6.3.[39] Mutations were performed by reading the new amino acid from the library in the $SP_AALIB directory, and superimposing the Cα–Cβ bond onto the wild-type residue based on Mackay's quaternion method. After performing the mutations, an extended conformation of the new residues in the Met113Phe$_7$ pore was obtained by rotating the β and γ carbons with the "tor" function of SPOCK. The model of TNT was produced with HyperChem 7.5 (Hypercube, Inc., Gainesville, FL, USA). After export as PDB files, representations of the mutant with bound TNT were produced with SPOCK and Adobe Photoshop.

Acknowledgements

Work at Texas A&M was supported by DARPA, the DoD Tri-Service Technology Program, DOE, NASA, NIH and ONR. H.B. is the holder of a Royal Society–Wolfson Research Merit Award and O.B. was supported by the Wellcome Trust.

Keywords: aromatic interactions · nanopores · protein engineering · sensors · single-molecule studies

[1] H. Bayley, O. Braha, L.-Q. Gu, *Adv. Mater.* **2000**, *12*, 139 – 142.
[2] H. Bayley, C. R. Martin, *Chem. Rev.* **2000**, *100*, 2575 – 2594.
[3] H. Bayley, P. S. Cremer, *Nature* **2001**, *413*, 226 – 230.
[4] O. Braha, B. Walker, S. Cheley, J. J. Kasianowicz, L. Song, J. E. Gouaux, H. Bayley, *Chem. Biol.* **1997**, *4*, 497 – 505.
[5] O. Braha, L.-Q. Gu, L. Zhou, X. Lu, S. Cheley, H. Bayley, *Nat. Biotechnol.* **2000**, *17*, 1005 – 1007.
[6] S. Cheley, L.-Q. Gu, H. Bayley, *Chem. Biol.* **2002**, *9*, 829 – 838.
[7] L.-Q. Gu, O. Braha, S. Conlan, S. Cheley, H. Bayley, *Nature* **1999**, *398*, 686 – 690.
[8] S.-H. Shin, T. Luchian, S. Cheley, O. Braha, H. Bayley, *Angew. Chem.* **2002**, *114*, 3859 – 3861; *Angew. Chem. Int. Ed.* **2002**, *41*, 3707 – 3709.
[9] S. Howorka, S. Cheley, H. Bayley, *Nat. Biotechnol.* **2001**, *19*, 636 – 639.
[10] L. Movileanu, S. Howorka, O. Braha, H. Bayley, *Nat. Biotechnol.* **2000**, *18*, 1091 – 1095.
[11] L. Song, M. R. Hobaugh, C. Shustak, S. Cheley, H. Bayley, J. E. Gouaux, *Science* **1996**, *274*, 1859 – 1865.
[12] L.-Q. Gu, S. Cheley, H. Bayley, *J. Gen. Physiol.* **2001**, *118*, 481 – 494.
[13] E. Moczydlowski in *Ion Channel Reconstitution* (Ed.: C. Miller), Plenum, New York, **1986**, pp. 75 – 113.
[14] D. A. Dougherty, *Science* **1996**, *271*, 163 – 168.
[15] M. Mascal, A. Armstrong, M. D. Bartberger, *J. Am. Chem. Soc.* **2002**, *124*, 6274 – 6276.
[16] G. B. McGaughey, M. Gagné, A. K. Rappé, *J. Biol. Chem.* **1998**, *273*, 15458 – 15463.
[17] R. Bhattacharyya, U. Samanta, P. Chakrabarti, *Protein Eng.* **2002**, *15*, 91 – 100.
[18] R. Bhattacharyya, R. P. Saha, U. Samanta, P. Chakrabarti, *J. Proteome Res.* **2003**, *2*, 255 – 263.
[19] P.-C. Hsu, M. R. Hodel, J. W. Thomas, L. J. Taylor, C. H. Hagedorn, A. E. Hodel, *Biochemistry* **2000**, *39*, 13730 – 13736.
[20] B. Hille, *Ion Channels of Excitable Membranes*, 3rd ed., Sinauer, Sunderland, MA, **2001**.
[21] O. Beckstein, M. S. P. Sansom, *Proc. Natl. Acad. Sci. USA* **2003**, *100*, 7063 – 7068.
[22] C. A. Hunter, K. R. Lawson, J. Perkins, C. J. Urch, *J. Chem. Soc. Perkin Trans. 2* **2001**, 651 – 669.
[23] M. L. Waters, *Curr. Opin. Chem. Biol.* **2002**, *6*, 736 – 741.
[24] E. A. Meyer, R. K. Castellano, F. Diederich, *Angew. Chem.* **2003**, *115*, 1244 – 1287; *Angew. Chem. Int. Ed.* **2003**, *42*, 1210 – 1250.
[25] S. K. Burley, G. A. Petsko, *Science* **1985**, *229*, 23 – 28.
[26] Agency for Toxic Substances and Disease Registry (ASTDR), *Toxicological Profile for 2,4,6-Trinitrotoluene (TNT)*, US Department of Health and Human Services, Public Health Service, **1995**.
[27] D. Bruns-Nagel, J. Breitung, E. von Löw, K. Steinbach, T. Gorontzy, M. Kahl, K.-H. Blotevogel, D. Gemsa, *Appl. Environ. Microbiol.* **1996**, *62*, 2651 – 2656.

[28] J.-S. Yang, T. M. Swager, *J. Am. Chem. Soc.* **1998**, *120*, 5321 – 5322.
[29] J.-S. Yang, T. M. Swager, *J. Am. Chem. Soc.* **1998**, *120*, 11 864 – 11 873.
[30] L. Chen, D. W. McBranch, H.-L. Wang, R. Helgeson, F. Wudl, D. G. Whitten, *Proc. Natl. Acad. Sci. USA* **1999**, *96*, 12 287 – 12 292.
[31] L. A. Pinnaduwage, A. Gehl, D. L. Hedden, G. Muralidharan, T. Thundat, R. T. Lareau, T. Sulchek, L. Manning, B. Rogers, M. Jones, J. D. Adams, *Nature* **2003**, *425*, 474.
[32] L. L. Looger, M. A. Dwyer, J. J. Smith, H. W. Hellinga, *Nature* **2003**, *423*, 185 – 190.
[33] T. A. Lewis, D. A. Newcombe, R. L. Crawford, *J. Environ. Manage.* **2004**, *70*, 291 – 307.
[34] C. A. Hunter, J. Singh, J. M. Thornton, *J. Mol. Biol.* **1991**, *218*, 837 – 846.
[35] L. Serrano, M. Bycroft, A. R. Fersht, *J. Mol. Biol.* **1991**, *218*, 465 – 475.
[36] R. Chelli, F. L. Gervasio, P. Procacci, V. Schettino, *Proteins* **2004**, *55*, 139 – 151.
[37] A. T. Brünger, D. J. Leahy, T. R. Hynes, R. O. Fox, *J. Mol. Biol.* **1991**, *221*, 239 – 256.
[38] G. Hu, P. D. Gershon, A. E. Hodel, F. A. Quiocho, *Proc. Natl. Acad. Sci. USA* **1999**, *96*, 7149 – 7154.
[39] J. A. Christopher, *SPOCK: The Structural Properties Observation and Calculation Kit (program manual)*, Center for Macromolecular Design, Texas A&M University, **1998**.

Received: February 12, 2005
Published online on August 24, 2005

